ORIGINAL RESEARCH

IL-1α Reversibly Inhibits Skeletal Muscle Ryanodine Receptor
A Novel Mechanism for Critical Illness Myopathy?

Oliver Friedrich[1,2,3]*, Bing Yi[2], Joshua N. Edwards[3], Barbara Reischl[1], Anette Wirth-Hücking[1], Andreas Buttgereit[1], Roland Lang[4], Cornelia Weber[2], Fabian Polyak[2], Ilon Liu[2], Frederic von Wegner[5], Tanya R. Cully[3], Aven Lee[3], Patrick Most[6], and Mirko Völkers[6]

[1]Institute of Medical Biotechnology, Friedrich-Alexander-University Erlangen-Nuremberg, Erlangen, Germany; [2]Institute of Physiology and Pathophysiology, Ruprecht-Karls-University, Heidelberg, Germany; [3]School of Biomedical Sciences, University of Queensland, St. Lucia, Brisbane, Queensland, Australia; [4]Institute of Microbiology and Infection Immunology, Friedrich-Alexander-University Erlangen-Nuremberg, Erlangen, Germany; [5]Brain Imaging Center, Goethe University, Frankfurt, Germany; and [6]Institute for Molecular and Translational Cardiology, Department of Internal Medicine III, University Clinics Heidelberg, Heidelberg, Germany

Abstract

Critical illness myopathies in patients with sepsis or sustained mechanical ventilation prolong intensive care treatment and threaten both patients and health budgets; no specific therapy is available. Underlying pathophysiological mechanisms are still patchy. We characterized IL-1α action on muscle performance in "skinned" muscle fibers using force transducers and confocal Ca^{2+} fluorescence microscopy for force/Ca^{2+} transients and Ca^{2+} sparks. Association of IL-1α with sarcoplasmic reticulum (SR) release channel, ryanodine receptor (RyR) 1, was investigated with coimmunoprecipitation and confocal immunofluorescence colocalization. Membrane integrity was studied in single, intact fibers challenged with IL-1α. IL-1α reversibly stabilized Mg^{2+} inhibition of Ca^{2+} release. Low Mg^{2+}–induced force and Ca^{2+} transients were reversibly abolished by IL-1α. At normal Mg^{2+}, IL-1α reversibly increased caffeine-induced force and Ca^{2+} transients. IL-1α reduced SR Ca^{2+} leak via RyR1, as judged by (*1*) increased SR Ca^{2+} retention, (*2*) increased IL-1α force transients being reproduced by 25 μM tetracaine, and (*3*) reduced Ca^{2+} spark frequencies by IL-1α or tetracaine. Coimmunoprecipitation confirmed RyR1/IL-1 association. RyR1/IL-1 immunofluorescence patterns perfectly colocalized. Long-term, 8-hour IL-1α challenge of intact muscle fibers compromised membrane integrity in approximately 50% of fibers, and confirmed intracellular IL-1α deposition. IL-1α exerts a novel, specific, and reversible interaction mechanism with the skeletal muscle RyR1 macromolecular release complex without the need to act via its membrane IL-1 receptor, as IL-1R membrane expression levels were not detectable in Western blots or immunostaining of single fibers. We present a potential explanation of how the inflammatory mediator, IL-1α, may contribute to muscle weakness in critical illness.

Keywords: cytokines; IL-1; ryanodine receptor 1; Ca^{2+} regulation; critical illness myopathy

Skeletal muscle is a very common target in inflammatory diseases. Increased proteolysis and muscle wasting is seen in tumor cachexia (1), chronic inflammation (2, 3), and critical illness (4, 5). Many patients in intensive care units (ICUs) develop sepsis and multiorgan failure. In many developed countries, sepsis ranks among conditions with the highest mortality (6). Most critically ill patients in the ICU develop neuromuscular dysfunctions (e.g., critical illness

(Received in original form February 6, 2013; accepted in final form December 23, 2013)

*O.F. is the senior author on this article.

This work was supported by the Deutsche Sepsis-Gesellschaft (O.F.), Australian Research Council grant LX0882427 (O.F.), German Research Foundation grants FR1499/7-1 (O.F.) and PM652/1-1 (P.M.), a CJ Martin Fellowship (J.N.E.), and National Institutes of Health grants RO1 HL92130 and RO1 HL92130-2S1 (P.M.).

Author Contributions: O.F. designed the entire study; P.M. and M.V. were involved in the study design; O.F., B.Y., C.W., and F.P. performed skinned fiber force recordings; O.F. and JNE performed single-fiber Ca^{2+} recordings; O.F. and F.v.W. performed and analyzed Ca^{2+} spark recordings; O.F., I.L., B.R., and A.B. performed and analyzed immunofluorescence experiments; O.F., T.R.C. performed and analyzed single-fiber cell culture experiments; O.F., B.R., A.W.-H., A.L., M.V., and P.M. performed and analyzed biochemistry experiments; O.F. analyzed force transducer and single fiber Ca^{2+} experiments; O.F. wrote the manuscript; all authors discussed and commented on the manuscript.

Correspondence and requests for reprints should be addressed to Oliver Friedrich, M.D., Institute of Medical Biotechnology, Friedrich-Alexander-University Erlangen-Nuremberg, Paul-Gordan-Straße 3, 91052 Erlangen, Germany. E-mail: oliver.friedrich@mbt.uni-erlangen.de

This article has an online supplement, which is accessible from this issue's table of contents at www.atsjournals.org

Am J Respir Cell Mol Biol Vol 50, Iss 6, pp 1096–1106, Jun 2014

Originally Published in Press as DOI: 10.1165/rcmb.2013-0059OC on January 8, 2014
Internet address: www.atsjournals.org

Clinical Relevance

Muscle weakness of the diaphragm and limb muscles is one of the most abundant complications in critically ill patients, which vastly prolongs treatment, intensive care unit stays, and health budgets. No specific cure is at hand, as the pathophysiology of the muscle weakness is still cryptic. This study describes a novel mechanism for inflammatory cytokine IL-1 action directed at the skeletal muscle ryanodine receptor to interfere with muscle activation and Ca^{2+} homeostasis. This IL-1 "off-receptor-site" target might be responsible to explain muscle dysfunction during inflammatory and critical illness myopathies. It also represents a unique, novel signaling property of this inflammatory mediator.

myopathies [CIMs]) that present with flaccid paralysis and impose vast threats to patients and health budgets. CIM is not restricted to sepsis, but can also be triggered by steroids or neuromuscular blockers (7, 8). Neuromuscular dysfunctions, such as seen in CIMs or critical illness polyneuropathies, are considered a form of organ failure secondary to critical illness, whether sepsis related or not (9).

Skeletal muscle is highly specialized and tuned for fast activation and force development. Action potentials spread along the sarcolemma and penetrate deep into the transverse tubules to activate dihydropyridine receptor (DHPR) voltage sensors. In skeletal muscle, DHPRs are conformationally coupled to sarcoplasmic ryanodine receptor (RyR) 1 Ca^{2+} release channels (10). Upon activation of DHPR, its II–III loop acutely lowers Mg^{2+} affinity of the inhibitory Mg^{2+} binding site on the RyR1 to enable sarcoplasmic reticulum (SR) Ca^{2+} release (11). Elevated myoplasmic Ca^{2+} activates cross-bridge cycling, force production, and motility. Apart from this "physiological activation" involving "Mg^{2+} disinhibition," the RyR1 contains a multitude of other regulatory binding sites (12). For example, methylxanthines (e.g., caffeine) increase Ca^{2+} affinity for the Ca^{2+} activation site, and induce strong SR Ca^{2+} release (13).

Cellular mechanisms of muscle failure in critical illness conditions are still poorly understood. Skeletal muscles mostly affected are limb muscles and the diaphragm, which translates to the symptoms seen in affected patients (i.e., acute quadriplegia or weaning failure [14]). Experimental approaches that cover the sepsis aspect of CIM range from LPS- (15) to cecal-ligation and puncture-induced sepsis (16), as well as acute septic serum challenge *in vitro* models (17), whereas other trigger factors apart from inflammation have been employed using steroid-denervation animal models (18). Although decreased membrane excitability (15, 18), decreased contractility and increased fatigability (16), or metabolic failure (19) have been noted across all different conditioning models, findings for altered Ca^{2+} homeostasis (20) have been only descriptive, and events that coin the mechanism of CIM have not been unraveled. During systemic inflammation, global and local cytokines are up-regulated (21). In mixed ICU patients, pro- and anti-inflammatory cytokines were vastly up-regulated in the blood, regardless of whether sepsis was present or not (22). In limb skeletal muscle biopsies from critically ill patients, vast immune cell infiltration and proinflammatory cytokine expression was detected (e.g., TNF-α and IL-1 [23]). This tempted us to investigate the role of selected cytokines on skeletal muscle dysfunction in a defined *in vitro* setting involving the extensor digitorum longus (EDL) muscle as a widely used fast-twitch–type limb muscle in muscle research. We chose IL-1 (IL-1α isoform; hereafter referred to as IL-1) as one prominent proinflammatory cytokine in sepsis and critical illness. Our results show a very unexpected and novel mechanism of IL-1–RyR1 interaction that may explain some aspects of muscle failure in conditions of CIM associated with high cytokine burden. This is the first demonstration of a direct cytokine action on a release channel that is not mediated via the cytokine receptor.

Materials and Methods

Force Transducer Recordings

Recordings were performed in small, C57Bl6 mouse EDL fiber bundles after chemical skinning (10 μg/ml saponin; 90 s) to gain diffusional access and control over the myoplasmic environment. Before global SR Ca^{2+} releases with either caffeine (30 mM) or introducing low-Mg^{2+} (10 μM) solution, SR was loaded in roughly 250 nM Ca^{2+}–containing internal solution. Force transients were recorded and amplitudes related to maximum force responses induced by high activating solution ($-\log(Ca^{2+})$ [pCa], ~ 4.2). pCa-force recordings were obtained in solutions with different pCas. IL-1 was added at 10, 25, or 100 ng/L before the releases for at least 1 minute (*see* Materials and Methods in the online supplement).

Confocal Ca^{2+} Recordings

Rhod-2 (10 μM) global Ca^{2+} transients were elicited in mechanically skinned single EDL fibers with caffeine or low Mg^{2+} with or without prior IL-1 incubation (25 ng/L). A complete sequence contained a control, an IL-1, and a final washout run. Ca^{2+} transients were analyzed from whole-fiber regions of interest of at least three individual single fibers. "Ca^{2+} sparks" were recorded in saponin-skinned single EDL fibers after staining with 10 μM Fluo-4. Confocal XYT series (100 frames at 0.9 frames per second) were taken under control conditions and 5 minutes after application of either IL-1 or tetracaine. Images were denoised and sparks detected using a wavelet-based technique and expressed as specific frequency. Further details are available in the Materials and Methods in the online supplement.

Immunofluorescence Recordings

Single saponin-skinned EDL fibers were incubated with 100 ng/L IL-1 for 1 hour to allow IL-1 to distribute inside the myoplasm. After fixation and applying an immunolabeling protocol for IL-1 and labeling RyR with Ry-BODIPY, sequential confocal 488 nm and 633 nm excitation fluorescence images were obtained (*see* the Materials and Methods in the online supplement).

IL-1 Incubation Cell Culture and Biochemistry Experiments

See the Materials and Methods in the online supplement for full details.

Results

IL-1 Reduces SR Ca^{2+} Leak by RyR1 Binding

In initial cytokine screens, IL-1 (10–100 ng/L) robustly and reversibly increased amplitudes

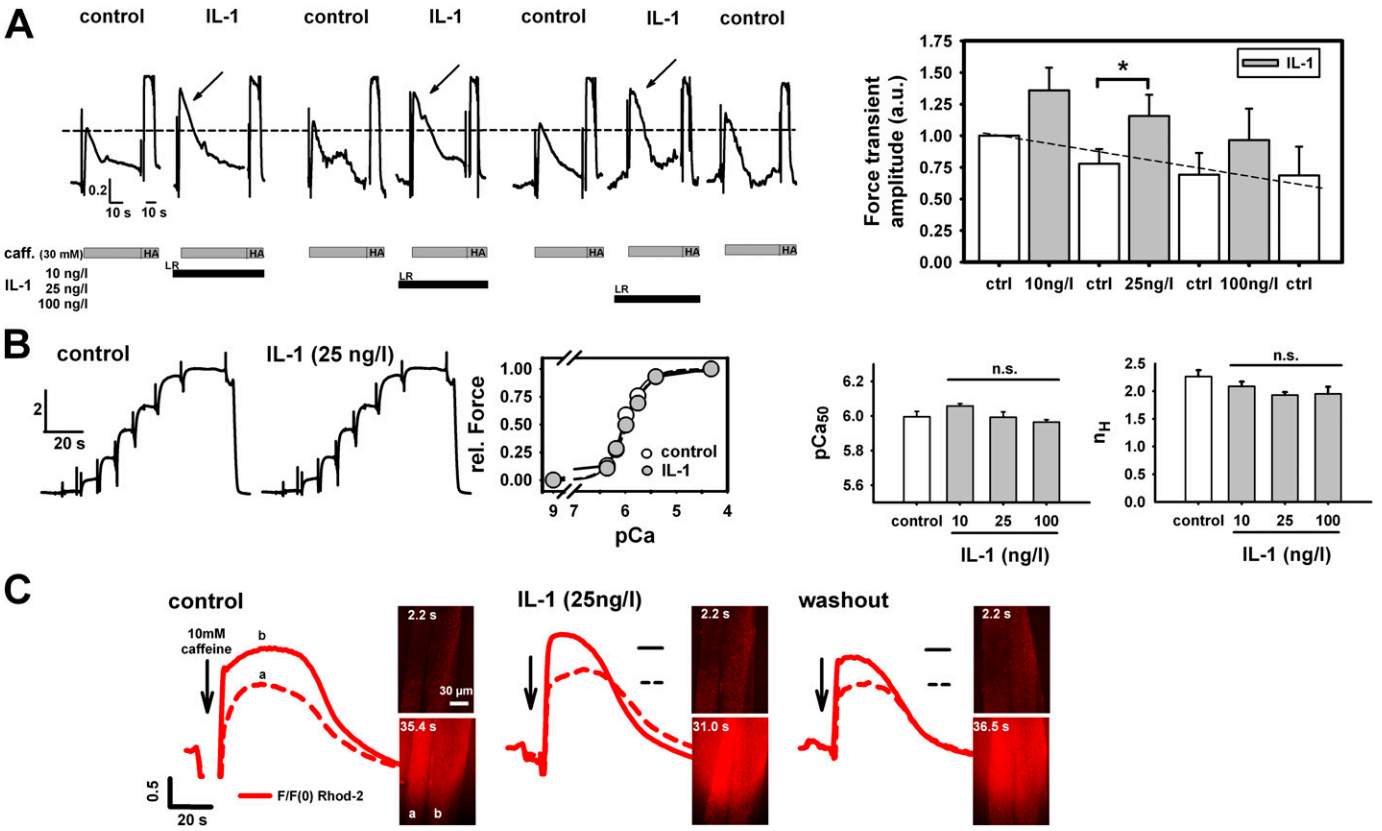

Figure 1. IL-1 directly increases caffeine-induced Ca^{2+} release in skeletal muscle. (*A*) Force transients in a skinned extensor digitorum longus (EDL) fiber bundle after incubation with different IL-1 concentrations. Force levels are consistently and reversibly increased by IL-1 (significant at 25 ng/L) and restored after washout. Maximum force (high-activating solution [HA]: $-\log[Ca^{2+}]$ [pCa], 4.2) is unaltered (*A*), as is Ca^{2+} sensitivity of the contractile apparatus (*B*; pCa_{50}, pCa for 50% force activation); n_H, Hill coefficient. n.s., not significant. (*C*) Direct confocal observation of caffeine-induced sarcoplasmic reticulum (SR) Ca^{2+} release in mechanically skinned single fibers confirms force transducer results. The *red cloud* reflects the global release of Ca^{2+} into the myoplasm and the surrounding solution. Sequences in (*A*) and (*C*) are from a single preparation (*horizontal lines* in [*C*], control levels). Similar results as in (*C*) were obtained in three preparations. $n = 5$ in (*A*) (*right panel*), n = 2–8 in (*B*). $^*P < 0.05$, ANOVA. LR, low relaxing solution. *Dashed lines* in (*A*) correspond to initial control peak force level (*left panel*) and projected linear run-down (*right panel*). *Dashed* and *solid lines* in (*C*) correspond to the amplitude of the control transients of fiber (a) and (b), respectively. caff., caffeine; F/F(0), fluorescence normalized to time point 0; rel. Force, relative force.

of caffeine-induced force transients without affecting maximum force level at pCa 4.2 (Figure 1A). The increase in force was significant at 25 ng/L, a concentration corresponding to plasma levels in septic shock (21). TNF-α failed to show such an effect (data not shown), and was not further pursued in this study. Ca^{2+} sensitivity of the contractile apparatus at any tested IL-1 concentration was unaffected (Figure 1B). Because this suggests that IL-1 increases SR Ca^{2+} release, we directly visualized myoplasmic Ca^{2+} in mechanically skinned single fibers (with the sarcolemma manually removed) by confocal microscopy as an independent validation and observed a reversible increase in Ca^{2+} fluorescence amplitude by IL-1 (Figure 1C). Because all fibers used were skinned, the IL-1–induced effect can be regarded as instantaneous, and does not involve IL-1 receptor (IL-1R) signaling, due to diffusional access to the myoplasm and full control of the intracellular milieu (i.e., all myoplasmic second messenger molecules removed by the artificial intracellular solution [> 1:1,000,000 dilution]). A more direct proof is shown in Figure E1 in the online supplement, where Western blots probing for IL-1R1 receptor subtype in small fiber bundles (Figure E1A), as well as immunostains in either chemically or mechanically skinned single fibers (Figure E1B), did not show any significant receptor expression levels in the muscle sarcolemma. We then tested whether the increased Ca^{2+} release observed by acute IL-1 incubation originated from a reduction of SR Ca^{2+} leak by IL-1 using a defined SR Ca^{2+} leak approach (24). Each cycle consists of 5-second–5-minute–5-second leak periods (the last one to check for reversibility) under control conditions after preincubation with IL-1 and washout (control) (Figure 2A). The relative decrease in force after prolonged leakage was substantially smaller with IL-1 than under control conditions, and was completely reversible (Ca^{2+} retention index; Figure 2C, paired experiments). During such long-lasting experiments (~ 80 min), maximum force levels remained stable under Ca^{2+} saturation conditions (pCa, 4.2). Even after tens of release-reloading cycles, caffeine-induced force was still larger with IL-1 in relation to maximum force than without IL-1 (Figure 2B). To elucidate the mechanism by which IL-1 interfered with SR Ca^{2+} leakage, we compared the action of IL-1 on caffeine-induced force transients with that of tetracaine, a known inhibitor of RyR1. In some experiments, tetracaine (25 μM) replaced IL-1. Again,

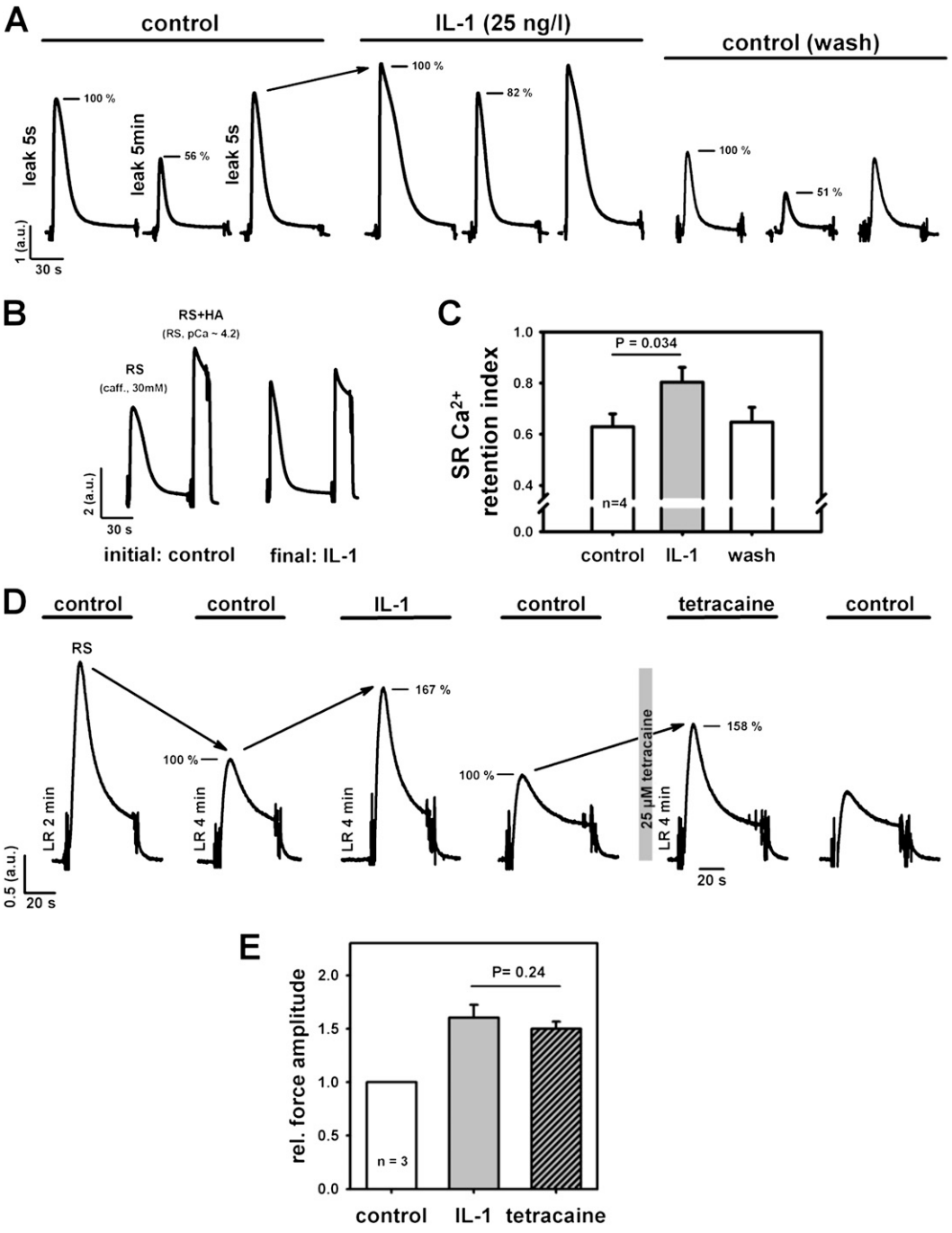

Figure 2. IL-1 increases SR Ca^{2+} by reducing SR Ca^{2+} leak through ryanodine receptor (RyR) 1. (*A*) Force recordings from one skinned EDL small fiber bundle to assess relative releasable SR Ca^{2+} content after leaking Ca^{2+} from the SR by defined incubation times. Extended leakage was completely reversible. Decrease in peak amplitude is reduced by IL-1. Note that the increase in force by IL-1 under identical conditions is robustly observed (e.g., last transient of control and first transient of IL-1, both 5-s leakage). (*B*) In long-lasting experiments (~80 min), relative increase of force amplitude after the final run was still very prominent and approached the maximum force at pCa 4.2. (*C*) Paired evaluation from four preparations confirms significant reduction in SR Ca^{2+} leak (i.e., larger SR Ca^{2+} retention index by IL-1). (*D*) Cycle of force transients aimed at identifying the source of IL-1 action at the SR. Two initial control releases after either 2- or 4-minute LR. Peak force amplitudes were compared between 4-minute LR control conditions (100%) and after either IL-1 (25 ng/L) or tetracaine preincubation. (*E*) The increase in force amplitude by IL-1 was mimicked by 25 μM tetracaine, indicating IL-1 binding to RyR1 to reduce SR Ca^{2+} leak. a.u., arbitray units; RS, release solution (LR + 30 mM caff.).

a robust and reversible increase in force was seen after IL-1 preincubation (25 ng/L; Figure 2D). After another control release, the next cycle included 25 μM tetracaine. This was completely reversible as well. Analysis from three such complete cycles revealed an almost identical increase in relative force (related to the previous control) by either IL-1 or tetracaine (Figure 2E). This strongly suggests

that IL-1 inhibits SR Ca^{2+} release by a robust and reversible RyR1 block.

As an independent test for this hypothesis, we recorded elementary Ca^{2+} release events (ECREs) as an indicator of RyR1 activity. With the SR loaded as in force recordings, a large number of ECREs was observed (Figure 3A). IL-1 reduced ECRE frequencies from approximately $15 \times 10^{-3}/100\ \mu m^2/s$ to approximately $4 \times 10^{-3}/100\ \mu m^2/s$ (unpaired analysis, $P < 0.01$; Figure 3B). In paired XYT recordings, relative spark frequency was decreased by roughly 75% ($P < 0.01$). This was mimicked by approximately 100 μM tetracaine ($n = 5$), in good agreement with the force data. Larger tetracaine concentrations reduced ECRE frequencies even further.

We next evaluated biochemical evidence for an association of IL-1 to RyR1. Intrinsic IL-1 was already detected in skeletal muscle homogenates (gastrocnemius, Figure 4A, EDL Figure 4D). Pulldown of IL-1 with subsequent immunoblotting for RyR1 showed substantial coimmunoprecipitation (Figure 4B). An immunoblot showing that the target protein (IL-1) was immunoprecipitated is shown in Figure 4C (control). The reverse procedure (immunoprecipitate [IP]:RyR, immunoblot:IL-1) confirmed this association (Figure 4D). To verify that the IL-1 band in the immunoblot of the IP: RyR assay indeed identified IL-1, another control probing for IL-1 in a blot running an IP:IL-1 on the recombinant IL-1α as input was additionally performed (Figure 4D). In contrast to the RyR1–IL-1 association, there was no association of IL-1 to sarco-endoplasmic reticulum Ca^{2+} ATPase (SERCA) (Figure 4D). We next performed confocal immunofluorescence experiments in single skinned EDL fibers after incubation with IL-1 to allow for RyR1 interaction. Both partners showed substantial overlap (Figures 4E and 4F). Striation pattern profiles and periodicity were virtually the same for IL-1 and RyR (Figures 4F and 4G). Spatial signal shifts between IL-1 and RyR1 signals for all maxima and minima were negligible (Figure 4H). These results show that the *in vitro* association translates to colocalization of IL-1 and RyR1 *in situ* within the resolution limits of the confocal microscope.

IL-1 Blocks Low Mg^{2+}–Induced Ca^{2+} Release

We suggest a reversible blocking action of IL-1 on the RyR1, which can still be overcome by the methylxanthine caffeine. However, normal muscle activation usually involves acute lowering of the RyR1 Mg^{2+} binding affinity in response to DHPR activation (11), thus relieving Mg^{2+} inhibition. Therefore, Mg^{2+} disinhibition of RyR1 in several fiber bundles was acutely induced by lowering cytoplasmic Mg^{2+}, yielding a short force transient (representative example shown in Figure 5A). After SR reloading and IL-1 preincubation, lowering Mg^{2+} failed to induce a force transient. Subsequent force transient after caffeine application ruled out compromised SR load (Figure 5A). A small force transient after IL-1 washout indicates recovery. As a last test to directly observe IL-1 washout on restoring the RyR1 Mg^{2+} site sensitivity toward low Mg^{2+}, in a different fiber bundle, Mg^{2+} was lowered in the presence of IL-1. Again, this prevented SR Ca^{2+} release. Then, only washing out IL-1 resulted in a prominent force transient (Figure 5A). To validate this observation directly for SR Ca^{2+} release,

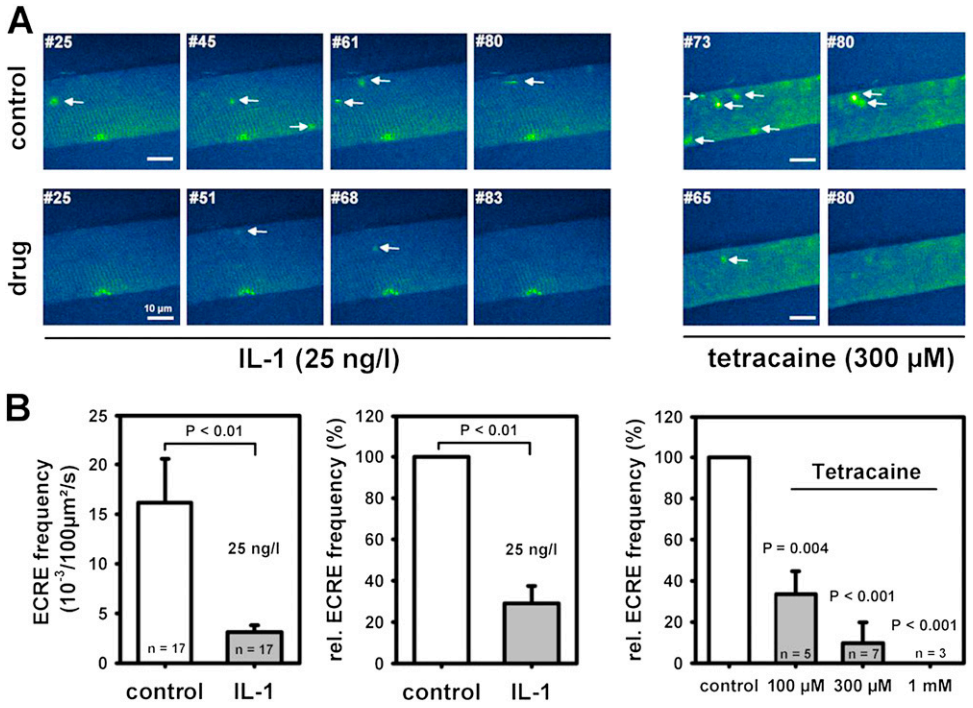

Figure 3. IL-1 partially blocks RyR1 and reduces Ca^{2+} spark frequencies in single skinned skeletal muscle fibers. (*A*) Images from XYT confocal Fluo-4 Ca^{2+} spark recordings of two single skinned EDL muscle fiber segments under control conditions and approximately 5 minutes after either application of 25 ng/L IL-1 or 300 μM tetracaine. Both drugs markedly reduced Ca^{2+} spark occurrence. Automated denoising and event detection allowed precise counts of Ca^{2+} sparks. *Arrows* represent detected sparks. *Scale bar*, 10 μm. (*B*) Ca^{2+} spark frequency was reduced approximately 75% by IL-1, and this corresponded to the effect exerted by approximately 100 μM tetracaine. ECRE, elementary Ca^{2+} release event.

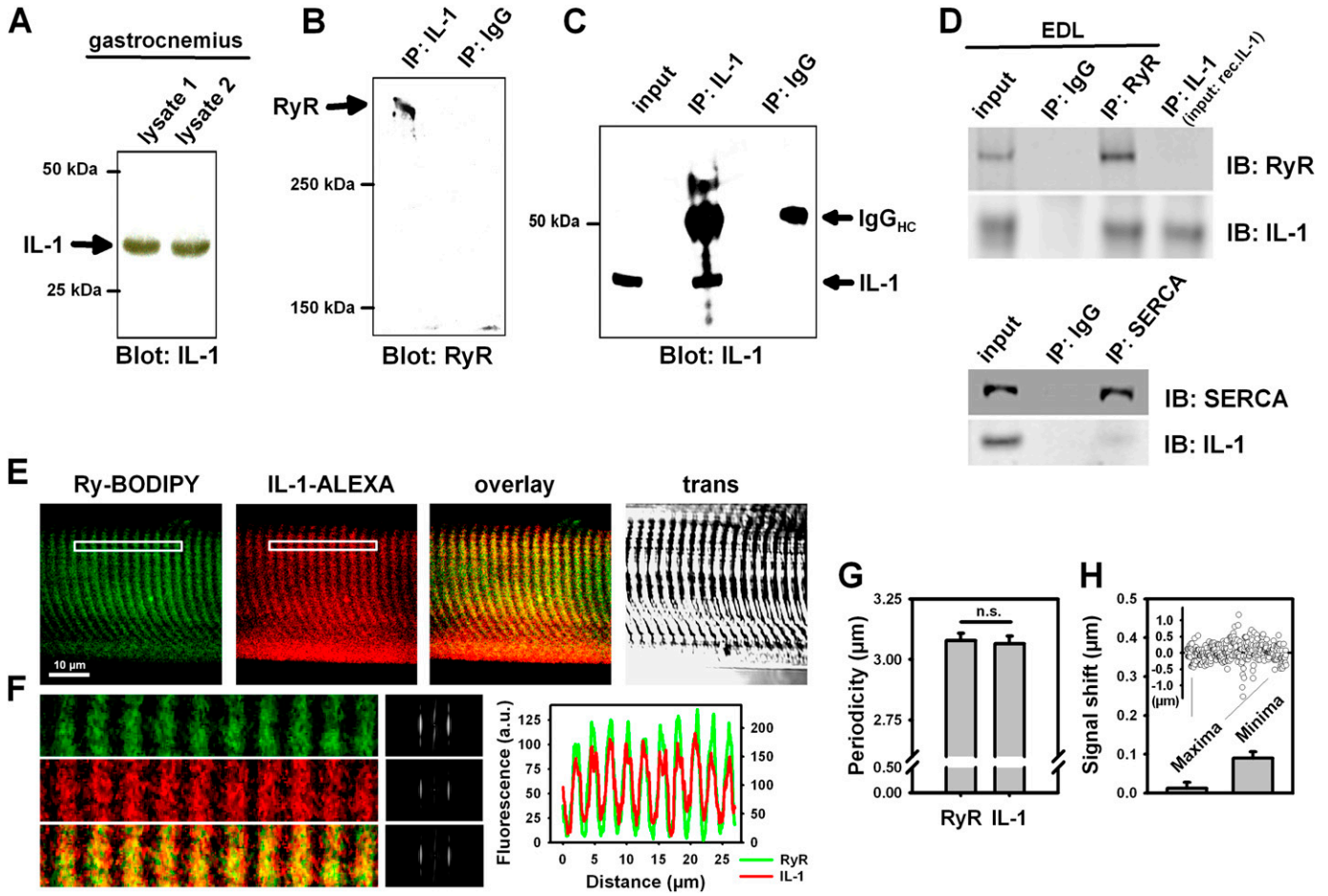

Figure 4. IL-1 coimmunoprecipitates and colocalizes with RyR1 in skeletal muscle. (*A*) Western blot demonstrating expression of IL-1 in gastrocnemius muscle; lysate samples (as indicated) were obtained from two independent control animals. (*B*) Coimmunoprecipitation of IL-1 and RyR in skeletal muscle: gastrocnemius lysate was incubated with anti–IL-1 antibody or IgG (control), precipitated using protein A beads and resolved on SDS-PAGE. Proteins were transferred to nitrocellulose membrane and probed with the antibodies against (*B*) RyR (immunoprecipitate [IP]:IL-1, immunoblot [IB]:RyR) or (*C*) IL-1 (IP:IL-1, IB:IL-1); RyR was detected as a band migrating at greater than 500 kD, but no signal was detected when lysates were incubated with the IgG control (IP:IgG, IB:RyR, IB:IL-1). (*D*) Co-IP of IL-1 and RyR in EDL skeletal muscle lysates using the reverse procedure as in (*B*) confirmed association of both proteins (IP:RyR, IB:IL-1). Unlike RyR, IL-1 did not coimmunoprecipitate with sarco-endoplasmic reticulum Ca^{2+} ATPase (SERCA; IP:SERCA, IB:IL-1). (*E*) Confocal immunofluorescence microscopy shows IL-1 and RyR colocalization *in situ* in permeabilized single EDL fibers after IL-1 incubation. (*F*) Magnification of the *boxed white area* in (*E*), the Fourier transforms of the periodic pattern, as well as the signal intensity overlay. (*G*) RyR1 and IL-1 periodicity patterns match perfectly. In addition, there is no shift in the maximum or minimum intensity of the spatial IL-1–to–RyR signal within the microscope resolution (*H*). IgG_{HC}, IgG heavy chain; rec.IL-1, recombinant IL-1; trans, transillumination image.

low Mg^{2+}–induced Ca^{2+} transients were tracked with the confocal microscope in the absence (control) or presence of IL-1, fully confirming the force recordings (Figure 5B). Because these findings were consistent in several preparations and independent methods, the effect seems to be robust.

IL-1 Compromises Membrane Integrity

Our data provide functional evidence for a selective RyR1 block by IL-1, most likely via stabilizing RyR1 Mg^{2+} inhibition. IL-1 usually acts through its plasmalemmal IL-1R (mostly the type I isoform), which was not detectable in our preparations (Figure E1). To be able to interact directly with RyR1, there must be a pathway for IL-1 to enter the cell, or IL-1 being overexpressed, or a combination of both. To address this possibility, we incubated and cultured intact single muscle cells in the presence of IL-1 for various durations. Subsequent staining with propidium iodide (PI) reveals compromised membrane integrity by IL-1 at concentrations from 25 ng/L starting after 4 hours (Figure 6A). These experiments show that IL-1 itself induces membrane leaks (by as yet unidentified mechanisms) that might serve as a pathway for this small signaling molecule to penetrate into the cell. Electrical excitability of PI-positive single fibers after 8-hour IL-1 incubation was qualitatively assessed with external field stimulation. About 30% of fibers responded with a twitch. Fibers that did not respond probably were already too depolarized (*see* DISCUSSION). To actually prove the presence of IL-1 in the muscle cells after prolonged IL-1 challenge, single intact muscle fibers were cocultured with IL-1 overnight ($\sim$ 10 h), washed (to completely remove external IL-1), and probed for IL-1 immunofluorescence. IL-1

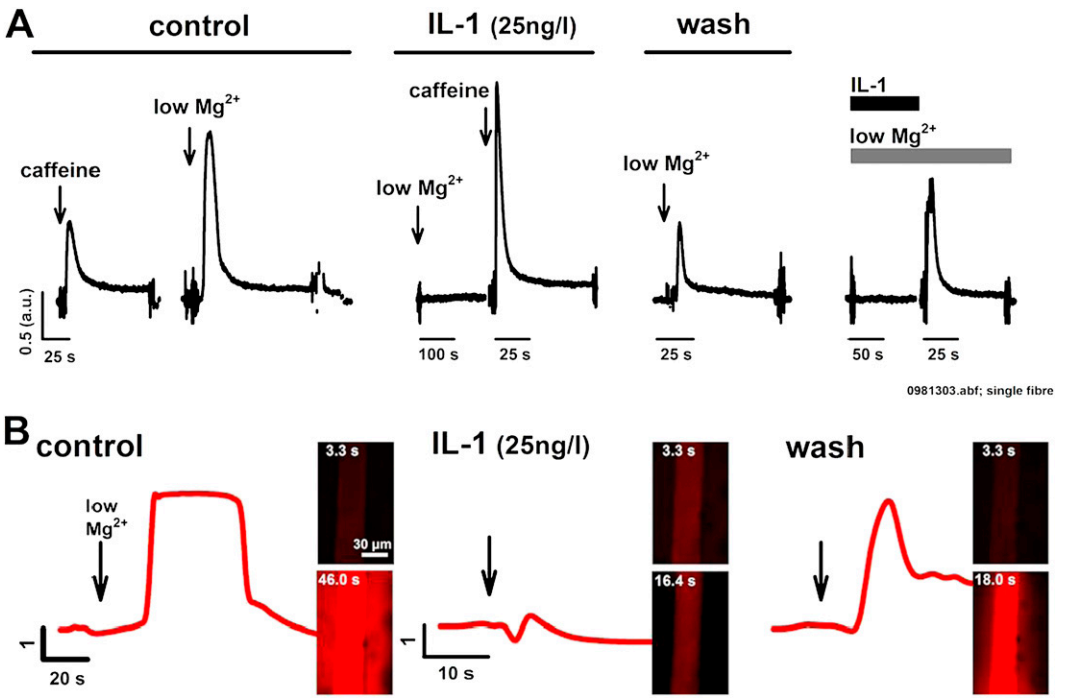

Figure 5. IL-1 reversibly blocks low Mg^{2+}–induced SR Ca^{2+} release. (*A*) Force transient recordings in two single muscle fibers under control caffeine and low Mg^{2+} conditions and after IL-1 preincubation. Low Mg^{2+} release was completely blocked by IL-1, but caffeine still induced a large release. After IL-1 washout and SR reloading with Ca^{2+}, low Mg^{2+} release was partially restored. In another preparation, while IL-1 was present, again, low Mg^{2+} did not induce Ca^{2+} release. After removal of IL-1, still in low Mg^{2+}, force transient was restored within seconds, while IL-1 diffused away from its binding partner into the bath solution. (*B*) Confocal Ca^{2+} transients in single, mechanically skinned fibers fully confirm the effect of IL-1 on blocking low Mg^{2+}–induced release, which, again, is partially reversible after IL-1 washout. Similar results were observed in three other preparations. abf, file extension of raw data file.

immunofluorescence was increased several fold in IL-1– treated fibers ($P < 0.01$; Figure 6B), thus confirming the intracellular presence of this cytokine.

Discussion

The main findings of the present study define a rather unexpected, novel mechanism for intracellular cytokine action that may explain some of the early muscle weakness and failure related to septic or other inflammatory myopathies, as well as nonseptic CIMs associated with increased cytokine profiles: (*1*) IL-1 (1α isoform) interacts with RyR1 *in situ* and *in vitro*; (*2*) IL-1 reduces SR Ca^{2+} leak through the RyR1 by stabilizing the Mg^{2+} inhibition; and (*3*) prolonged IL-1 incubation of intact muscle fibers compromises membrane integrity to provide a potential penetration pathway. That indeed SR Ca^{2+} release was affected by IL-1 was shown by the unaltered Ca^{2+} sensitivity of the contractile apparatus by IL-1 in the force transducer assay, and also directly by confocal Ca^{2+} fluorescence experiments. The effects of IL-1 on SR Ca^{2+} release were almost instantaneous and reversible once IL-1 interacted with RyR1 in the skinned fiber assay. This is not in contrast to the long incubation times needed for intact fibers to exert the action of IL-1 on membrane integrity, as, in the skinned fiber, the sarcolemma had been permeabilized either chemically or mechanically and immediate diffusional access to the myoplasm established (25). Physiological Ca^{2+} release occurs via DHPR–RyR1 interaction to reduce the Mg^{2+} affinity of RyR1 and, thus, disinhibition of Mg^{2+} block (11). Depolarization of the t-system and DHPR activation is a rather strong stimulus to open RyR1 (26). In the skinned fiber, this can be mimicked by acutely lowering myoplasmic Mg^{2+} concentration (25), although this is a somewhat milder stimulus for release (26). In our hands, lowering Mg^{2+} produced robust Ca^{2+} and force transients, which were completely and reversibly abolished in the presence of IL-1. The fact that caffeine could still induce SR Ca^{2+} release is reflected by caffeine (at 30 mM) strongly increasing the Ca^{2+} affinity on the RyR1 activation site (27). An explanation for the increase in caffeine-induced force levels after IL-1 incubations is most likely reflected by a reduced SR Ca^{2+} leak and consequent larger releasable SR Ca^{2+} pools. Apart from RyR1, SR Ca^{2+} leakage is also possible via the SERCA, particularly in heart muscle (28), whereas, in skeletal muscle, SR Ca^{2+} leak seems predominantly via RyR1 (29) or a recently described transient receptor channel, transient receptor potential canonical type 1 pathway (30). The fact that the SR Ca^{2+} retention index (24) increase and the spark frequency decrease upon IL-1 application were well reproduced by tetracaine, together with the finding that IL-1 coimmunoprecipitated with RyR1, but not with SERCA (Figure 4), clearly point toward RyR1 as the main target for this cytokine. Tetracaine has been used in previous studies in muscle to block spark frequencies (i.e., 6-fold reduction at 75–100 μM [31]), or caffeine-induced force transients (32). As pointed out by Pike and colleagues (32), tetracaine action strongly depends on both drug concentrations and

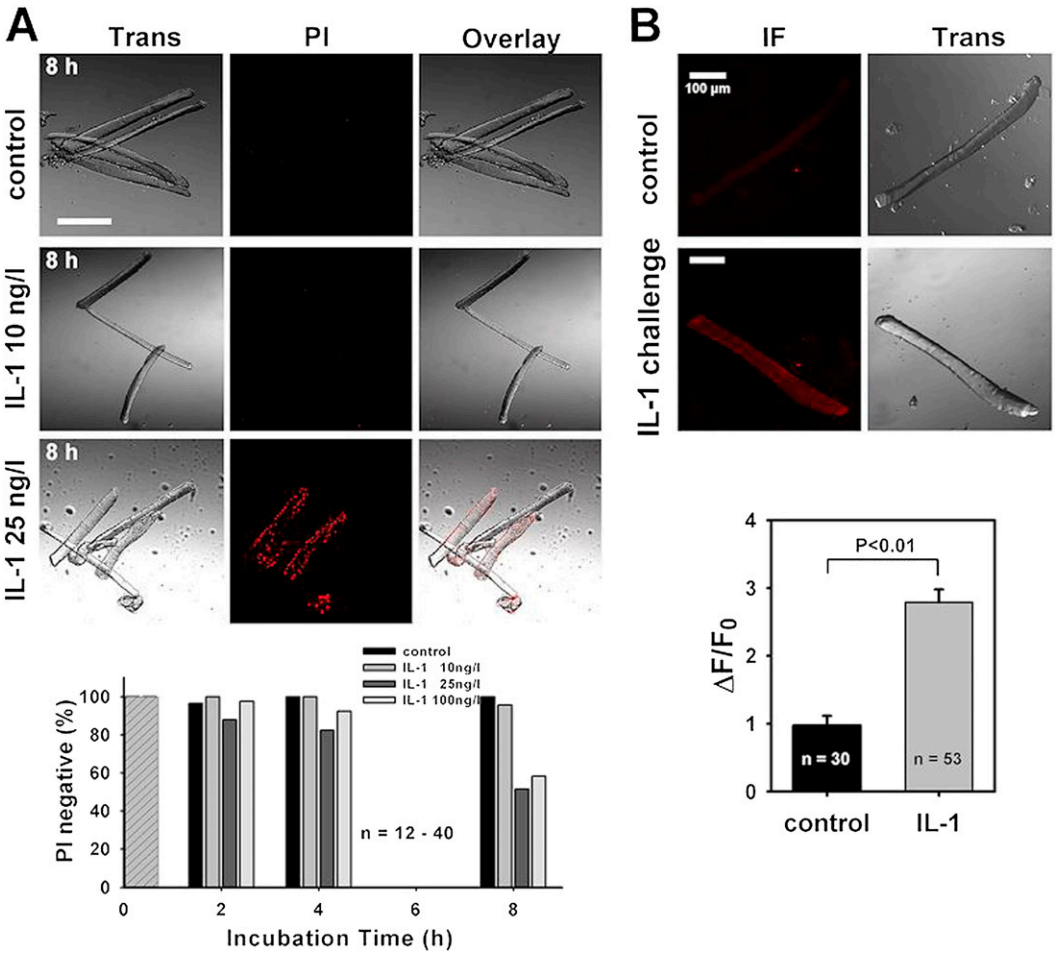

Figure 6. Prolonged IL-1 exposure compromises muscle membrane integrity to provide an IL-1 entry pathway. (*A*) Propidium iodide (PI) staining after 8-hour challenge with IL-1 shows compromised membrane integrity at 25 ng/L. From 25 ng/L, approximately 50% of cells are PI positive after 8 hours (30% of which responded to external field stimulation with a twitch). (*B*) After overnight IL-1 incubation (25 ng/L), almost no IL-1 fluorescence was seen in control cells, but substantial IL-1 signal was detected in IL-1–challenged cells, proving that IL-1 was located inside the fibers ($P < 0.01$, ANOVA). *Scale bars*, 100 μm. $\Delta F/F_0$, relative fluorescence change normalized to initial fluorescence at time point 0; IF, immunofluorescence; Trans, transillumination image.

pCa. In particular, our combination of incubation and washout times eliminated persistent blocking effects of tetracaine between recordings.

Concentration Effects of IL-1 and Potential Relations to Sepsis and Inflammatory Myopathies

The effects of IL-1 were most prominent at 25 ng/L, a concentration intriguingly reflecting blood levels found in patients with sepsis, whereas 10 ng/L typically correspond to healthy individuals (21, 33). In patients with sepsis who developed myopathy, substantial tissue infiltrates with macrophages and high local IL-1 expression patterns have been detected (21), pointing toward a required precondition for IL to invade individual muscle cells to exert the pathophysiological effects documented in the present study. Indeed, the compromised membrane integrity after long-term IL-1 incubation might be sufficient to provide an uptake pathway for this relatively small molecule by endocytosis, diffusion, or some other, yet to be determined transport mechanism. In diaphragm muscle, experimental sepsis increased the percentage of myofibers with compromised membrane integrity from less than 1% to up to 20%, whereas no effect was observed in soleus muscle (34, 35). Interestingly, in cultured cerebromicrovascular endothelial cells, an IL-1R–dependent transport mechanism of IL-1 across cell membranes has been suggested (36). Whether a similar, IL-1R–dependent mechanism also applies to skeletal muscle would be most interesting to address in future studies involving, for example, IL-1R–deficient mice (37). Both Western blots of small fiber bundles and immunostaining of chemically or mechanically skinned single EDL fibers could not detect any specific IL-1R1 protein expression. In muscle biopsies from patients with idiopathic inflammatory myopathies, Grundtman and colleagues (38) described IL-1R1 and IL-1R2 expression in muscle histology sections at the level of the sarcolemma and the nuclei. However, because no single fibers were employed, signal contributions from immune cell infiltrates in the interstitial space cannot be excluded. Because the mechanically skinned fiber allowed the comparison of IL-1R1 signals both from the unskinned (still sarcolemma containing) and the skinned side of the "cuff," we can confidently say that IL-1R1 expression levels,

if present, are below the detection limit of the Western blot and immunostaining performed, which confirms previous results (39). Finally, it is also possible that immune activation of the skeletal muscle inflammasome with secretion of IL-1 (40) may additionally contribute to the internal deposition of IL-1, as detected by our long-term overnight challenge of intact single fibers.

To the best of our knowledge, this is the very first study systematically investigating the action of the cytokine, IL-1α, on skeletal muscle Ca^{2+} homeostasis. Studies involving isolated cytokines or cytokine cocktails are important, yet very scarce for skeletal muscle. Probably best studied is the proinflammatory cytokine, TNF-α, incubation of which with intact diaphragm and limb muscle (flexor digitorum brevis [FDB]) fibers for 4 hours produced substantial decrement in tetanic force without altering underlying Ca^{2+} transients. Thus, it was concluded that TNF-α somehow reduced myofilament sensitivity toward Ca^{2+} (41). In C_2C_{12} skeletal myotubes incubated with TNF-α for a 48-hour period, however, the opposite effect had been observed (i.e., TNF-α markedly depressed electrically evoked Ca^{2+} transients [42]). It is very likely that some of the multiple suggested slow signaling mechanisms involved in cytokine-mediated muscle weakness (reactive oxygen species, nitric oxide production, peroxidation, ATP depletion [5]) respond differentially to different prolonged *exposure time* versus *concentration* products. However, in the case of IL-1α in our study, it is highly unlikely that second messenger–related pathways contributed significantly to the observed effects in our skinned fiber preparation, where the myoplasmic environment is in equilibrium with a defined *indefinite* bath volume controlling the fiber cytosol, and no longer containing signaling molecules in any significant amounts (calculated dilution $>1{:}10^6$). Therefore, the documented IL-1 effects are likely to be direct and are almost completely reversible. In the heart, IL-1 has been used to elucidate mechanisms of cardiac failure in models of septic cardiomyopathy. A very recent study showed that a 3-hour treatment of rat cardiomyocytes significantly reduced Ca^{2+} transients, fractional shortening, and SR Ca^{2+} content, but only when cells were cocultured with TNF-α (43). Either cytokine on its own only induced minor changes. However, IL-1 concentrations were approximately 100-fold higher compared with those used in our studies. Under these conditions, the authors deduced increased SR Ca^{2+} leak from increased spark frequencies in the presence of cytokines, in contrast to our findings in skeletal muscle and at more clinically relevant concentrations.

A New Model Explaining Critical Illness and Inflammatory Myopathies?

We suggest a new model that may explain some aspects of early muscle failure and weakness in critically ill patients, in particular in conditions involving a strong inflammatory response. Systemic inflammation is associated with leukocytosis and local tissue infiltration by immune cells (23). Activated macrophages secrete IL-1 (mostly IL-1β, but also the IL-1α isoform) into the muscle tissue, accumulating high tissue levels. As critical illness progresses, patient muscle fibers may become exposed to high local concentrations of IL-1 (23). In time, muscle membrane integrity is compromised, providing a passage for IL-1 to enter myocytes. These transient membrane leaks will be repaired by most cells (44), but also allow entry of cations and subsequent membrane depolarization that additionally interfere with muscle performance (45). This also explains why not all single fibers were still electrically excitable after extended IL-1 challenge. In addition, activated inflammasome also increases IL-1 expression within muscle cells (40). All this would enable IL-1 to associate with RyR1 within the cell, by-passing the usual IL-1R–mediated signaling cascade (46), or using it for IL-1R–mediated IL-1 entry (36) if surface receptors were present at large enough densities. Given sufficient repair mechanisms of the membrane after localized membrane damage (44), a general Ca^{2+} overload of muscle fibers and subsequent cell death seems unlikely. IL-1 bound to the RyR1 macromolecular complex then stabilizes Mg^{2+} inhibition of SR Ca^{2+} release, representing a reversible block of the release channel. Although reduced SR Ca^{2+} leak via RyR1 stabilizes or may even increase SR Ca^{2+} content, RyR1 inhibition remains during the course of cytokine burden. Our acute IL-1 assay was almost completely reversible in terms of the SR effects. However, this may be more puzzling in the critically ill patient. Prolonged sepsis, for example, induced vast ultrastructural changes to muscle architecture by selective proteolysis of myofilaments (47, 48). Some of these effects can be triggered by isolated cytokines (47). Although proteolysis is already stimulated within hours after mechanical ventilation (49) or sepsis (48), and can be just as rapidly reversible, it is probably the altered contractile architecture as a consequence of maintained proteolysis in ongoing critical illness that leads to sarcomere disruptions (50) and even "ghost sarcomeres" with selective myosin loss (48). The latter might be reversible only at a much longer time scale, and may be responsible for structurally related contractile dysfunction. Indeed, patients with myosin loss myopathy in CIMs usually take months to recover (51).

Past clinical studies employing anti–IL-1 therapy did not show any benefit for patients with sepsis, despite most promising results in rodents (52). However, all those studies explored *mortality* as the endpoint to evaluate treatment efficiency rather than muscle function. Thus, whether anti–IL-1 treatment would be able to improve muscle function or prevent/ameliorate CIM would be an interesting hypothesis for future studies. ■

Author disclosures are available with the text of this article at www.atsjournals.org.

References

1. Tisdale MJ. Mechanisms of cancer cachexia. *Physiol Rev* 2009;89: 381–410.
2. Steffen BT, Lees SJ, Booth FW. Anti-TNF treatment reduces rat skeletal muscle wasting in monocrotaline-induced cardiac cachexia. *J Appl Physiol* 2008;105:1950–1958.
3. Langen RC, Schols AM, Kelders MC, Wouters EF, Janssen-Heininger YM. Inflammatory cytokines inhibit myogenic differentiation through activation of nuclear factor-kappaB. *FASEB J* 2001;15: 1169–1180.
4. Larsson L. Experimental animal models of muscle wasting in intensive care unit patients. *Crit Care Med* 2007;35: S484–S487.

5. Reid MB, Campbell IT, Little RA. Muscle wasting and energy balance in critical illness. *Clin Nutr* 2004;23:273–280.
6. Engel C, Brunkhorst FM, Bone HG, Brunkhorst R, Gerlach H, Grond S, Gruendling M, Huhle G, Jaschinski U, John S, *et al*. Epidemiology of sepsis in Germany: results from a national prospective multicenter study. *Intensive Care Med* 2007;33:606–618.
7. Horinouchi H, Kumamoto T, Kimura N, Ueyama H, Tsuda T. Myosin loss in denervated rat soleus muscle after dexamethasone treatment. *Pathobiology* 2005;72:108–116.
8. Larsson L, Li X, Edstrom L, Eriksson LI, Zackrisson H, Argentini C, Schiaffino S. Acute quadriplegia and loss of muscle myosin in patients treated with nondepolarizing neuromuscular blocking agents and corticosteroids: mechanisms at the cellular and molecular level. *Crit Care Med* 2000;28:34–45.
9. Friedrich O. Critical illness myopathy: sepsis-related failure of the peripheral nervous system. *Eur J Anaesthesiol* 2008;42:73–82.
10. Stange M, Tripathy A, Meissner G. Two domains in dihydropyridine receptor activate the skeletal muscle Ca(2+) release channel. *Biophys J* 2001;81:1419–1429.
11. Haarmann CS, Dulhunty AF, Laver DR. Regulation of skeletal ryanodine receptors by dihydropyridine receptor II–III loop C-region peptides: relief of Mg^{2+} inhibition. *Biochem J* 2005;387:429–436.
12. Lehnhart SE. Novel targets for treating heart and skeletal muscle disease—stabilizing ryanodine receptors and preventing intracellular calcium leak. *Curr Opin Pharmacol* 2007;7:225–232.
13. Murayama T, Kurebayashi N, Ogawa Y. Role of Mg^{2+} in Ca^{2+}-induced Ca^{2+} release through ryanodine receptors of frog skeletal muscle: modulations by adenine nucleotides and caffeine. *Biophys J* 2000; 78:1810–1824.
14. Bolton CF. Neuromuscular manifestations of critical illness. *Muscle Nerve* 2005;32:140–163.
15. Haeseler G, Foadi N, Wiegand E, Ahrens J, Krampfl K, Dengler R, Leuwer M. Endotoxin reduces availability of voltage-gated human skeletal muscle sodium channels at depolarized membrane potentials. *Crit Care Med* 2008;36:1239–1247.
16. Rossignol B, Gueret G, Pennec JP, Morel J, Rannou F, Giroux-Metges MA, Talamin H, Gioux M, Arvieux CC. Effects of chronic sepsis on contractile properties of fast twitch muscle in an experimental model of critical illness neuromyopathy in the rat. *Crit Care Med* 2008;36: 1855–1863.
17. Friedrich O, Hund E, Weber C, Hacke W, Fink RHA. Critical illness myopathy serum fractions affect membrane excitability and intracellular calcium release in mammalian skeletal muscle. *J Neurol* 2004;254:53–65.
18. Filatov GN, Rich MM. Hyperpolarization shifts in the voltage dependence of fast inactivation of Nav1.4 and Nav1.5 in a rat model of critical illness myopathy. *J Physiol* 2004;559:813–820.
19. Vanhorebeek I, De Vos R, Mesotten D, Wouters PJ, De Wolf-Peeters C, van den Berghe G. Protection of hepatocyte mitochondrial ultrastructure and function by strict blood glucose control with insulin in critically ill patients. *Lancet* 2005;365:53–59.
20. Zink W, Kaess M, Hofer S, Plchky J, Zausig YA, Sinner B, Weigand MA, Fink RH, Graf BM. Alterations in intracellular Ca^{2+}-homeostasis of skeletal muscle fibres during sepsis. *Crit Care Med* 2008;36: 1559–1563.
21. Joulin O, Petillot P, Labalette M, Lancel S, Neviere R. Cytokine profile of human septic shock serum inducing cardiomyocyte contractile dysfunction. *Physiol Res* 2007;56:291–297.
22. Dimopoulou I, Orfanos S, Kotanidou A, Livaditi O, Giamarellos-Bourboulis E, Athanasiou C, Korovesi I, Sotiropoulou C, Kopterides P, Ilias I, *et al*. Plasma pro- and anti-inflammatory cytokine levels and outcome prediction in unselected critically ill patients. *Cytokine* 2008;41:263–267.
23. De Letter MAC, van Doorn PA, Savelkoul HFJ, Laman JD, Schmitz PIM, Op de Coul AAW, Visser LH, Kros JM, Teepen JLJM, van der Meche FGA. Critical illness polyneuropathy and myopathy (CIPNM): evidence for local immune activation by cytokine-expression in the muscle tissue. *J Neuroimmunol* 2000;106:206–213.
24. Launikonis BS, Stephenson DG. Effect of saponin treatment of the sarcoplasmic reticulum of rat, cane toad and crustacean (yabby) skeletal muscle. *J Physiol* 1997;504:425–437.
25. Pedersen TH, Nielsen OB, Lamb GD, Stephenson DG. Intracellular acidosis enhances the excitability of working muscle. *Science* 2004; 305:1144–1147.
26. Lamb GD, Cellini MA, Stephenson DG. Different Ca^{2+} releasing action of caffeine and depolarization in skeletal muscle fibres of the rat. *J Physiol* 2001;531:715–728.
27. Laver DR, O'Neill ER, Lamb GD. Luminal Ca^{2+}-regulated Mg^{2+} inhibition of skeletal RyRs reconstituted as isolated channels or coupled clusters. *J Gen Physiol* 2004;124:741–758.
28. Kuum M, Kaasik A, Joubert F, Ventura-Clapier R, Veksler V. Energetic state is a strong regulator of sarcoplasmic reticulum Ca^{2+} loss in cardiac muscle: different efficiencies of different energy sources. *Cardiovasc Res* 2009;83:89–96.
29. Eltit JM, Yang T, Li H, Molinski TF, Pessah IN, Allen PD, Lopez JR. RyR1-mediated Ca^{2+} leak and Ca^{2+} entry determine resting intracellular Ca^{2+} in skeletal myotubes. *J Biol Chem* 2010;285: 13781–13787.
30. Berbey C, Weiss N, Legrand C, Allard B. Transient receptor potential canonical type 1 (TRPC1) operates as a sarcoplasmic reticulum calcium leak channel in skeletal muscle. *J Biol Chem* 2009;284: 36387–36394.
31. Hollingworth S, Chandler WK, Baylor SM. Effects of tetracaine on voltage-activated calcium sparks in frog intact skeletal muscle fibers. *J Gen Physiol* 2006;127:291–307.
32. Pike GK, Abramson JJ, Salama G. Effects of tetracaine and procaine on skinned muscle fibres depend on free calcium. *J Muscle Res Cell Motil* 1989;10:337–349.
33. Gogos CA, Drosou E, Bassaris HP, Skoutelis A. Pro- versus anti-inflammatory cytokine profile in patients with severe sepsis: a marker for prognosis and future therapeutic options. *J Infect Dis* 2000;181: 176–180.
34. Supinski GS, Callahan LA. Free radical–mediated skeletal muscle dysfunction in inflammatory conditions. *J Appl Physiol* 2007;102: 2056–2063.
35. Lin MC, Ebihara S, El Dwairi Q, Hussain SNA, Yang L, Gottfried SB, Comtois A, Petrof BJ. Diaphragm sarcolemmal injury is induced by sepsis and alleviated by nitric oxide synthase inhibition. *Am J Respir Crit Care Med* 1998;158:1656–1663.
36. Skinner RA, Gibson RM, Rothwell NJ, Pinteaux E, Penny JI. Transport of interleukin-1 across cerebromicrovascular endothelial cells. *Br J Pharmacol* 2009;156:1115–1123.
37. Kish DD, Gorbachev AV, Fairchild RL. IL-1 receptor signaling is required at multiple stages of sensitization and elucidation of the contact hypersensitivity response. *J Immunol* 2012;188:1761–1771.
38. Grundtman C, Salomonsson S, Dorph C, Bruton J, Andersson U, Lundberg IE. Immunolocalization of interleukin-1 receptors in the sarcolemma and nuclei of skeletal muscle in patients with idiopathic inflammatory myopathies. *Arthritis Rheum* 2007;56:674–687.
39. Zhang Y, Pilon G, Marette A, Baracos VE. Cytokines and endotoxin induce cytokine receptors in skeletal muscle. *Am J Physiol Endocrinol Metab* 2000;279:E196–E205.
40. Rawat R, Cohen TV, Ampong B, Francia D, Henrique-Pons A, Hoffman EP, Nagaraju K. Inflammasome up-regulation and activation in dysferlin-deficient skeletal muscle. *Am J Pathol* 2010;176: 2891–2900.
41. Reid MB, Lännergren J, Westerblad H. Respiratory and limb muscle weakness induced by tumor necrosis factor-α. *Am J Respir Crit Care Med* 2004;166:479–484.
42. van Kann LN, Bakker AJ. Effect of tumor necrosis factor α on electrically induced calcium transients elicited in C2C12 skeletal myotubes. *Muscle Nerve* 2007;35:251–253.
43. Duncan DJ, Yang Z, Hopkins PM, Steele DS, Harrison SM. TNF-alpha and IL-1beta increase Ca^{2+} leak from the sarcoplasmic reticulum and susceptibility to arrhythmia in rat ventricular myocytes. *Cell Calcium* 2010;47:378–386.
44. Cai C, Weisleder N, Ko JK, Komazaki S, Sunada Y, Nishi M, Takeshima H, Ma J. Membrane repair defects in muscular dystrophy are linked to altered interaction between MG53, caveolin-3, and dysferlin. *J Biol Chem* 2009;284:15894–15902.
45. Leon A, Boczkowski J, Dureui B, Desmonts JM, Aubier M. Effects of endotoxin shock on diaphragmatic function in mechanically ventilated rats. *J Appl Physiol* 1992;72:1466–1472.

46. Kim SJ, Choi Y, Jun HS, Kim BM, Na HK, Surh YJ, Park T. High-fat diet stimulates IL-1 type I receptor–mediated inflammatory signaling in the skeletal muscle of mice. *Mol Nutr Food Res* 2010; 54:1014–1020.
47. Li YP, Reid MBNF. NF-kappaB mediates the protein loss induced by TNF-alpha in differentiated skeletal muscle myotubes. *Am J Physiol Regul Integr Comp Physiol* 2000;279:R1165–R1170.
48. Williams AB, Decourten-Myers GM, Fischer JE, Luo G, Sun X, Hasselgren PO. Sepsis stimulates release of myofilaments in skeletal muscle by a calcium-dependent mechanism. *FASEB J* 1999;13: 1435–1443.
49. DeRuisseau KC, Kavazis AN, Deering MA, Falk DJ, van Gammeren D, Yimlamai T, Ordway GA, Powers SK. Mechanical ventilation induces alterations of the ubiquitin-proteasome pathway in the diaphragm. *J Appl Physiol* 2004;98:1314–1321.
50. Powers SK, Wiggs MP, Sollanek KJ, Smuder AJ. Ventilator-induced diaphragm dysfunction: cause and effect. *Am J Physiol Regul Integr Comp Physiol* 2013;305(5):R464–R477.
51. Latronico N, Shehu I, Seghelini E. Neuromuscular sequelae of critical illness. *Curr Opin Crit Care* 2005;11:381–390.
52. Webster NR, Galley HF. Immunomodulation in the critically ill. *Br J Anaesth* 2009;103:70–81.